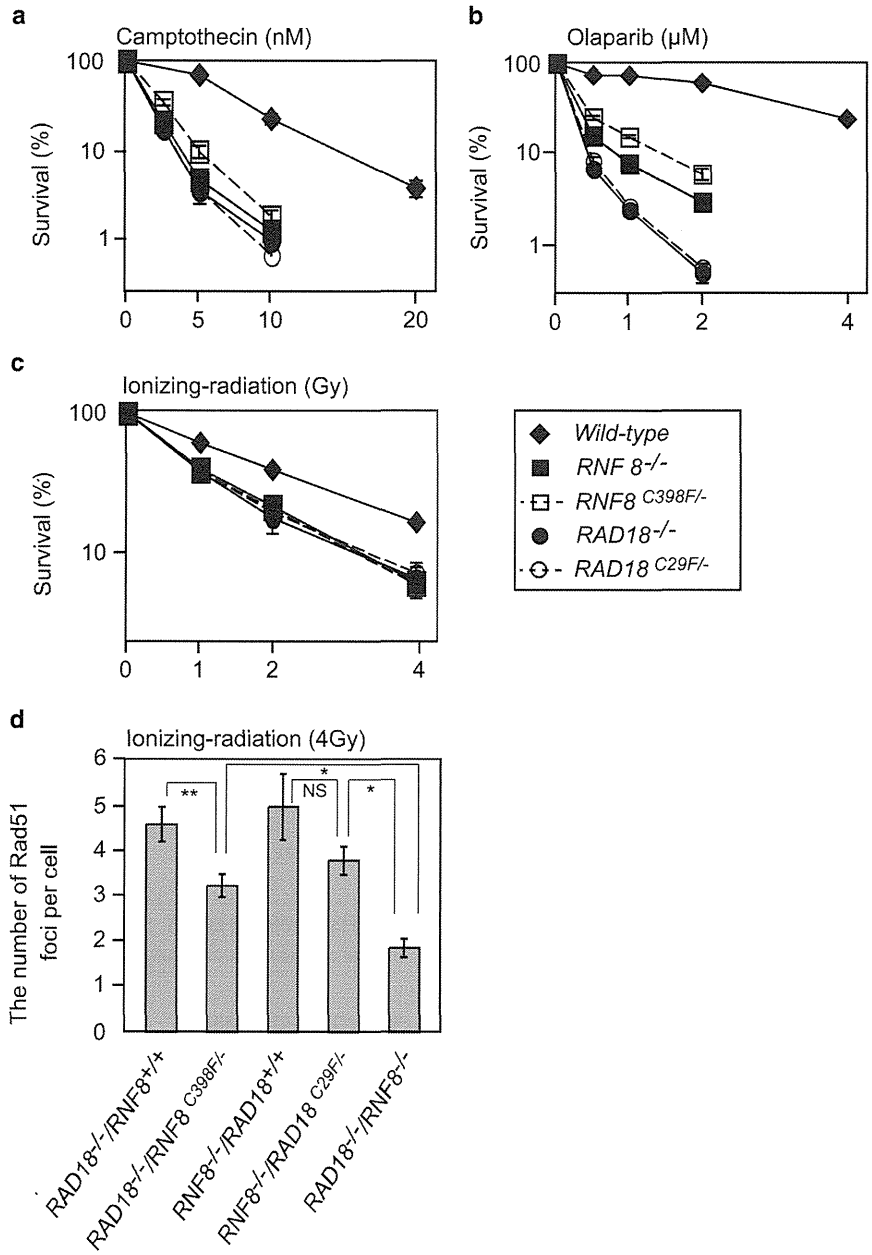

Figure 4. The ubiquitylation activity of Rad18 and Rnf8 is essential for cellular tolerance to camptothecin, olaparib and ionizing radiation. (**a**–**c**) Cellular sensitivity to camptothecin (**a**), olaparib (**b**) and ionizing radiation (**c**) is shown as in Figure 1. Error bars represent the s.e. of the mean in at least three independent experiments. (**d**) The average number of Rad51 foci at 1 h after γ-ray irradiation. More than 100 cells were counted in each experiment and the data represent the mean and s.e. from at least three independent experiments. $^{*}P < 0.01$, $^{**}P < 0.05$ and NS (not significant).

tolerance to camptothecin and olaparib. The rationale for this is because 53BP1 and Ku80 could repress an initial step of HR, whereas Rad18 and Rnf8 inhibit the toxic effect of NHEJ on HR without affecting Rad51 focus formation (Figure 3d). Future studies are required to identify substrates for ubiquitylation as well as the structure of ubiquitylation at various DNA lesions.

MATERIALS AND METHODS

Plasmid construction

For disrupting the *RNF8* gene, *RNF8-puro*, *RNF8-bsr* and *RNF8-neo* were generated from genomic PCR products using the primers 5′-GTA ACTGTAGGCCGGGGATTAGATCTCACG-3′ and 5′-CGGCTCAGTTCTTCC ATCAGAGCATGATGC-3′. Amplified PCR products were cloned into the pCRII-TOPO vector (Invitrogen, Carlsbad, CA, USA). The 5.3-kb *Xba*I fragment from the cloned PCR amplified region was further subcloned into the *Xba*I site of the pBluescriptII KS (+) vector. Each marker gene cassette was ligated into the *Bam*HI site that corresponds to the 86th amino-acid residue of the *RNF8* coding sequence. The 1.2-kb fragment from genomic DNA amplified using the primers 5′-GCATCATGCTCT GATGGAAGAACTGAGCCG-3′ and 5′-GCAATAATGGTGGGAACTGCACATG TGGAG-3′ was used as a probe for Southern blot analysis. The expression of *RNF8* mRNA was detected by reverse transcription-PCR using the primers 5′-GGCGGCATGGCAGCGTGCGGTGCCTCGAG-3′ and 5′-TTA CACTGTTTAGATAACGCAGTAGCTTCC-3′. Each *RAD18* C29F and *RNF8*

C398F knock-in vector was generated from genomic PCR using the following primers.

For *RAD18* C29F,
5′-AGTCAGAAATAAGCGTGGGTGGATATCCGT-3′
5′-GCTGAAGTAATCGAAG***A***AAATCCCACAGC-3′ for left arm,
5′-GCTGTGGGATTT***T***CTTCGATTACTTCAGC-3′
5′-CTGGCAGAACTGAAGCTCTTCACTAGCTC-3′ for right arm.

Amplified PCR products were cloned into pCR-Blunt II-TOPO vector (Invitrogen). The *Eco*RI fragment from this vector was further subcloned into the *Not*I site of the pBluescriptII KS (+) vector. *Not*I site of this vector was used to clone a marker gene (*puro*) cassette.

For *RNF8* C398F,
5′-GGAGTAAAATGGAAAGATGGGGAAGAGAAT-3′
5′-GCTCAGAACAGATTGTG***A***ACTGCAGCTC-3′ for left arm,
5′-GAGCTGCAGT***T***CACAATCTGTTCTGAGC-3′
5′-TTAGATAACGCAGTAGCTTCCATTAT-3′ for right arm.

Amplified PCR products were cloned into pCR-Blunt II-TOPO vector (Invitrogen). *Sca*I site was used to clone a marker gene (*puro*) cassette.

To detect full-length *RNF8* and *RAD18* mRNAs, following primers were used.

For *RNF8*,
5′-ATGGCAGCGTGCGGTGCCTCGAGGCC-3′
5′-TTAGATAACGCAGTAGCTTCCATTAT-3′.

For *RAD18*,
5′-ATGGCCCTGGCGCTGCCCGAACCGC-3′
5′-TCAGCTCTTCTTCCTCTTGCTCCTG-3′.

For the detection of *PCNA* mRNA,
5′-GGGATGTTTGAGGCGCGGCTTGT-3′
5′-CCTCAGTCCCAGTGCAGTTAAGA-3′.

Generation of *RNF8*$^{-/-}$, *RNF8*$^{-/-}$/*KU70*$^{-/-}$, *RAD18*$^{-/-}$/*RNF8*$^{-/-}$, *RAD18* C29F and *RNF8* C398F knock-in mutants

Wild-type DT40 cells were sequentially transfected with the *RNF8-bsr* and the *RNF8-puro* targeting constructs to obtain *RNF8*$^{-/-}$ cells. The gene-targeting frequency of the stably transfected clones was 50% for the *RNF8*$^{-/+}$ cells and 20% for the *RNF8*$^{-/-}$ clones. The *RNF8-puro* and the *RNF8-neo* targeting constructs were sequentially transfected into *KU70*$^{-/-}$ cells to obtain *RNF8*$^{-/-}$/*KU70*$^{-/-}$ cells. *RAD18*$^{-/-}$cells were sequentially transfected with the *RNF8-bsr* and the *RNF8-puro* targeting constructs to obtain *RAD18*$^{-/-}$/*RNF8*$^{-/-}$ cells. The establishment of each mutant was confirmed by Southern blotting. To establish *RAD18* C29F and *RNF8* C398F knock-in mutants, each construct described above was transfected into *RAD18*$^{+/-}$ (and *RNF8*$^{-/-}$/*RAD18*$^{+/-}$) or *RNF8*$^{+/-}$(and *RAD18*$^{-/-}$/ *RNF8*$^{+/-}$), respectively, and then gene targeting was validated by PCR. To remove the resistant gene, cells were transfected with the Cre recombinase expression vector and then treated with 0.2 μM tamoxifen. Forty-eight hours after the treatment, cells were subcloned and puromycin-sensitive clones were selected.

Chromosome aberration analysis

Karyotype analysis was performed as described previously.[34] For the morphological analysis of chromosome aberrations, cells were treated with colcemid for 3 h to enrich for mitotic cells. To count camptothecin-induced chromosomal aberrations, cells were treated with 10 or 100 nM camptothcin for 8h and colcemid was added in the last 3 h.

Measurement of cellular sensitivity to DNA-damaging agents

We measured the amount of ATP in cellular lysates to determine the number of live cells.[35] Cells were treated with each DNA-damaging agent in 1 ml of medium using 24-well plates and incubated at 39.5 °C for 48 h (or 72 h for olaparib). We transferred 100 μl of medium containing the cells to 96-well plates and measured the amount of ATP using CellTiter-Glo (Promega, Madison, WI, USA) according to the manufacturer's instructions. Luminescence was measured by Fluoroskan Ascent FL (Thermo Fisher Scientific Inc., Pittsburgh, PA, USA) or ARVO X5 (Perkin Elmer Inc., Branchburg, NJ, USA).

Immunofluorescent visualization of subnuclear focus formation

The experimental conditions for the immunocytochemical analysis were previously described.[28] Briefly, 30 min for FK2 or 1 h for Rad51 after irradiation with ^{137}Cs γ-ray (4 Gy) or after exposure to camptothecin (40 nM) for 1 h, DT40 cells (7×10^5 cells/ml) were collected on a glass slide using Cytospin3 (Shandon, Pittsburgh, PA, USA). Cells were fixed with 4% formaldehyde for 10 min at room temperature. After blocking with 3% bovine serum albumin/phosphate-buffered saline with Tween-20, the fixed cells were treated with specific antibodies. Visualization of the Rad51 and FK2 foci was performed as previously described, using the anti-Rad51 rabbit polyclonal antibody (Bioacademia Inc., Osaka, Japan) or the mouse FK2 antibody (Nippon Biotest Laboratories, Tokyo, Japan). At least 100 morphologically intact cells were examined.

Human HCT116 cells were grown on coverslips and then washed twice with phosphate-buffered saline before fixation. The cells were fixed with 3% paraformaldehyde and permeabilized with 0.5% Triton-X-100/phosphate-buffered saline. After blocking with 3% goat serum/phosphate-buffered saline, the cells were stained with a Rad51 rabbit polyclonal and a 53BP1 mouse monoclonal antibody (BD Bioscience, San Jose, CA, USA) at 4 °C overnight. For secondary staining, we used a goat Alexa555 anti-rabbit (Invitrogen) and a goat Alexa488 anti-mouse antibody (Invitrogen). The DNA was stained with 4′,6-diamidino-2-phenylindole. The coverslips were mounted with Prolong Gold mounting agent (Invitrogen).

siRNA transfection

The following siRNAs were used in this study: control (MISSION SIC-002, Sigma Genosys, Tokyo, Japan), RNF8 (Thermo Fisher Scientific Inc.) and BRCA1 5′-GGA ACC UGU CUC CAC AAA GTT-3′ (Sigma Genosys). RNA interference transfection for RNF8 and BRCA1 was performed using Lipofectamin RNAiMAX (Invitrogen) in reverse transfection mode.

Western blot analysis of monoubiquitylation of PCNA

For the detection of PCNA monoubiquitylation, 1×10^7 cells were irradiated with 30 J/m^2 UV and lysed 1.5 h post treatment with Laemli sample buffer and 5% 2-ME and then boiled for 5 min followed by ice incubation. The sample (10 μl) was run in an SDS–polyacrylamide electrophoresis gel and then proteins were electroblotted onto a polyvinylidene fluoride membrane. The following antibodies were used: mouse monoclonal PCNA PC10 (Santa Cruz, Santa Cruz, CA, USA) and anti-mouse IgG HRP liked (Santa Cruz). Proteins were visualized by Chemi-Lumi One Super (Nacalai Tesque, Inc., Kyoto, Japan).

CONFLICT OF INTEREST

The authors declare no conflict of interest.

ACKNOWLEDGEMENTS

This work was supported in part by the grants-in-aid program of the Ministry of Education, Sports and Culture of Japan (for ST). We thank Drs Tadahiro Shiomi and Naoko Shiomi (National Institute of Radiological Sciences, Japan) for providing us with the HCT116 *RAD18*$^{-/-}$ and *RAD18*$^{+/+}$ cells and Professor Hitoshi Kurumizaka (Waseda University, Japan) for providing us with the anti-Rad51 antibody. Financial support was provided in part by the Uehara Memorial Foundation, the Naito Foundation, Sumitomo Foundation and Kurata Fundation (for KH).

REFERENCES

1 Yamashita YM, Okada T, Matsusaka T, Sonoda E, Zhao GY, Araki K *et al.* RAD18 and RAD54 cooperatively contribute to maintenance of genomic stability in vertebrate cells. *EMBO J* 2002; **21**: 5558–5566.
2 Yoshimura A, Nishino K, Takezawa J, Tada S, Kobayashi T, Sonoda E *et al.* A novel Rad18 function involved in protection of the vertebrate genome after exposure to camptothecin. *DNA Repair (Amst)* 2006; **5**: 1307–1316.
3 Saberi A, Hochegger H, Szuts D, Lan L, Yasui A, Sale JE *et al.* RAD18 and poly(ADP-ribose) polymerase independently suppress the access of nonhomologous end joining to double-strand breaks and facilitate homologous recombination-mediated repair. *Mol Cell Biol* 2007; **27**: 2562–2571.
4 Takata M, Sasaki MS, Sonoda E, Morrison C, Hashimoto M, Utsumi H *et al.* Homologous recombination and non-homologous end-joining pathways of DNA double-strand break repair have overlapping roles in the maintenance of chromosomal integrity in vertebrate cells. *EMBO J* 1998; **17**: 5497–5508.
5 Pommier Y. Topoisomerase I inhibitors: camptothecins and beyond. *Nat Rev* 2006; **6**: 789–802.
6 Bryant HE, Schultz N, Thomas HD, Parker KM, Flower D, Lopez E *et al.* Specific killing of BRCA2-deficient tumours with inhibitors of poly(ADP-ribose) polymerase. *Nature* 2005; **434**: 913–917.

7 Adachi N, So S, Koyama H. Loss of nonhomologous end joining confers camptothecin resistance in DT40 cells. Implications for the repair of topoisomerase I-mediated DNA damage. *J Biol Chem* 2004; **279**: 37343–37348.
8 Farmer H, McCabe N, Lord CJ, Tutt AN, Johnson DA, Richardson TB *et al.* Targeting the DNA repair defect in BRCA mutant cells as a therapeutic strategy. *Nature* 2005; **434**: 917–921.
9 Hochegger H, Dejsuphong D, Fukushima T, Morrison C, Sonoda E, Schreiber V *et al.* Parp-1 protects homologous recombination from interference by Ku and Ligase IV in vertebrate cells. *EMBO J* 2006; **25**: 1305–1314.
10 Bunting SF, Callen E, Wong N, Chen HT, Polato F, Gunn A *et al.* 53BP1 inhibits homologous recombination in Brca1-deficient cells by blocking resection of DNA breaks. *Cell* 2010; **141**: 243–254.
11 Li L, Halaby MJ, Hakem A, Cardoso R, El Ghamrasni S, Harding S *et al.* Rnf8 deficiency impairs class switch recombination, spermatogenesis, and genomic integrity and predisposes for cancer. *J Exp Med* 2010; **207**: 983–997.
12 Santos MA, Huen MS, Jankovic M, Chen HT, Lopez-Contreras AJ, Klein IA *et al.* Class switching and meiotic defects in mice lacking the E3 ubiquitin ligase RNF8. *J Exp Med* 2010; **207**: 973–981.
13 Lu LY, Wu J, Ye L, Gavrilina GB, Saunders TL, Yu X. RNF8-dependent histone modifications regulate nucleosome removal during spermatogenesis. *Dev Cell* 2010; **18**: 371–384.
14 Sun J, Yomogida K, Sakao S, Yamamoto H, Yoshida K, Watanabe K *et al.* Rad18 is required for long-term maintenance of spermatogenesis in mouse testes. *Mech Dev* 2009; **126**: 173–183.
15 Wu J, Chen Y, Lu LY, Wu Y, Paulsen MT, Ljungman M *et al.* Chfr and RNF8 synergistically regulate ATM activation. *Nat Struct Mol Biol* 2011; **18**: 761–768.
16 Zhao GY, Sonoda E, Barber LJ, Oka H, Murakawa Y, Yamada K *et al.* A critical role for the ubiquitin-conjugating enzyme Ubc13 in initiating homologous recombination. *Mol Cell* 2007; **25**: 663–675.
17 Yamazoe M, Sonoda E, Hochegger H, Takeda S. Reverse genetic studies of the DNA damage response in the chicken B lymphocyte line DT40. *DNA Repair (Amst)* 2004; **3**: 1175–1185.
18 Yamamoto M, Okamoto T, Takeda K, Sato S, Sanjo H, Uematsu S *et al.* Key function for the Ubc13 E2 ubiquitin-conjugating enzyme in immune receptor signaling. *Nat Immunol* 2006; **7**: 962–970.
19 Fukushima T, Matsuzawa S, Kress CL, Bruey JM, Krajewska M, Lefebvre S *et al.* Ubiquitin-conjugating enzyme Ubc13 is a critical component of TNF receptor-associated factor (TRAF)-mediated inflammatory responses. *Proc Natl Acad Sci USA* 2007; **104**: 6371–6376.
20 Adachi N, Suzuki H, Iiizumi S, Koyama H. Hypersensitivity of nonhomologous DNA end-joining mutants to VP-16 and ICRF-193: implications for the repair of topoisomerase II-mediated DNA damage. *J Biol Chem* 2003; **278**: 35897–35902.
21 Maede Y, Shimizu H, Fukushima T, Kogame T, Nakamura T, Miki T *et al.* Differential and common DNA repair pathways for topoisomerase I- and II-targeted drugs in a genetic DT40 repair cell screen panel. *Mol Cancer Ther* 2014; **13**: 214–220.
22 Oestergaard VH, Pentzold C, Pedersen RT, Iosif S, Alpi A, Bekker-Jensen S *et al.* RNF8 and RNF168 but not HERC2 are required for DNA damage-induced ubiquitylation in chicken DT40 cells. *DNA Repair (Amst)* 2012; **11**: 892–905.
23 Mailand N, Bekker-Jensen S, Faustrup H, Melander F, Bartek J, Lukas C *et al.* RNF8 ubiquitylates histones at DNA double-strand breaks and promotes assembly of repair proteins. *Cell* 2007; **131**: 887–900.
24 Kolas NK, Chapman JR, Nakada S, Ylanko J, Chahwan R, Sweeney FD *et al.* Orchestration of the DNA-damage response by the RNF8 ubiquitin ligase. *Science* 2007; **318**: 1637–1640.
25 Huen MS, Grant R, Manke I, Minn K, Yu X, Yaffe MB *et al.* RNF8 transduces the DNA-damage signal via histone ubiquitylation and checkpoint protein assembly. *Cell* 2007; **131**: 901–914.
26 Huang J, Huen MS, Kim H, Leung CC, Glover JN, Yu X *et al.* RAD18 transmits DNA damage signalling to elicit homologous recombination repair. *Nat Cell Biol* 2009; **11**: 592–603.
27 Luijsterburg MS, Acs K, Ackermann L, Wiegant WW, Bekker-Jensen S, Larsen DH *et al.* A new non-catalytic role for ubiquitin ligase RNF8 in unfolding higher-order chromatin structure. *EMBO J* 2012; **31**: 2511–2527.
28 Takata M, Sasaki MS, Tachiiri S, Fukushima T, Sonoda E, Schild D *et al.* Chromosome instability and defective recombinational repair in knockout mutants of the five Rad51 paralogs. *Mol Cell Biol* 2001; **21**: 2858–2866.
29 Lu CS, Truong LN, Aslanian A, Shi LZ, Li Y, Hwang PY *et al.* The RING finger protein RNF8 ubiquitinates Nbs1 to promote DNA double-strand break repair by homologous recombination. *J Biol Chem* 2012; **287**: 43984–43994.
30 Inagaki A, van Cappellen WA, van der Laan R, Houtsmuller AB, Hoeijmakers JH, Grootegoed JA *et al.* Dynamic localization of human RAD18 during the cell cycle and a functional connection with DNA double-strand break repair. *DNA Repair (Amst)* 2009; **8**: 190–201.
31 Chapman JR, Taylor MR, Boulton SJ. Playing the end game: DNA double-strand break repair pathway choice. *Mol Cell* 2012; **47**: 497–510.
32 Watanabe K, Iwabuchi K, Sun J, Tsuji Y, Tani T, Tokunaga K *et al.* RAD18 promotes DNA double-strand break repair during G1 phase through chromatin retention of 53BP1. *Nucleic Acids Res* 2009; **37**: 2176–2193.
33 Palle K, Vaziri C. Rad18 E3 ubiquitin ligase activity mediates Fan coni anemia pathway activation and cell survival following DNA Topoisomerase 1 inhibition. *Cell Cycle* 2011; **10**: 1625–1638.
34 Sonoda E, Sasaki MS, Buerstedde JM, Bezzubova O, Shinohara A, Ogawa H *et al.* Rad51-deficient vertebrate cells accumulate chromosomal breaks prior to cell death. *EMBO J* 1998; **17**: 598–608.
35 Ji K, Kogame T, Choi K, Wang X, Lee J, Taniguchi Y *et al.* A novel approach using DNA-repair-deficient chicken DT40 cell lines for screening and characterizing the genotoxicity of environmental contaminants. *Environ Health Perspect* 2009; **117**: 1737–1744.

Supplementary Information accompanies this paper on the Oncogene website (http://www.nature.com/onc)

Journal of Steroid Biochemistry & Molecular Biology 139 (2014) 61–72

Contents lists available at ScienceDirect

Journal of Steroid Biochemistry and Molecular Biology

journal homepage: www.elsevier.com/locate/jsbmb

Estrogen Response element-GFP (ERE-GFP) introduced MCF-7 cells demonstrated the coexistence of multiple estrogen-deprivation resistant mechanisms

Natsu Fujiki[a,1], Hiromi Konno[a,1], Yosuke Kaneko[a], Tatsuyuki Gohno[a], Toru Hanamura[a], Koshi Imami[d], Yasushi Ishihama[e], Kyoko Nakanishi[f], Toshifumi Niwa[a], Yuko Seino[a,c], Yuri Yamaguchi[c], Shin-ichi Hayashi[a,b,*]

[a] Department of Molecular and Functional Dynamics, Tohoku University Graduate School of Medicine, Aoba-ku, Sendai 980-8575, Japan
[b] Center for Regulatory Epigenomics and Diseases, Tohoku University Graduate School of Medicine, Aoba-ku, Sendai 980-8575, Japan
[c] Research Institute for Clinical Oncology, Saitama Cancer Center, Ina-machi, Saitama 362-0806, Japan
[d] Institute for Advanced Biosciences, Keio University, Daihoji, Tsuruoka, Yamagata 997-0017, Japan
[e] Graduate School of Pharmaceutical Sciences, Kyoto University, Sakyo-ku, Kyoto 606-8501, Japan
[f] Institute of Medicinal Molecular Design, Inc. (IMMD), 5-24-5 Hongo, Bunkyo-ku, Tokyo 113-0033, Japan

ARTICLE INFO

Article history:
Received 20 May 2013
Received in revised form 17 August 2013
Accepted 20 August 2013

Keywords:
Estrogen
Breast cancer
Hormonal therapy
Estrogen-deprivation resistance

ABSTRACT

The acquisition of estrogen-deprivation resistance and estrogen receptor (ER) signal-independence in ER-positive breast cancer is one of the crucial steps in advancing the aggressiveness of breast cancer; however, this has not yet been elucidated in detail. To address this issue, we established several estrogen-deprivation-resistant (EDR) breast cancer cell lines from our unique MCF-7 cells, which had been stably transfected with an ERE-GFP reporter plasmid. Three cell lines with high ER activity and another 3 cell lines with no ER activity were established from cell cloning by monitoring GFP expression in living cells. The former three ERE-GFP-positive EDR cell lines showed the overexpression of ER and high expression of several ER-target genes. Further analysis of intracellular signaling factors revealed a marked change in the phosphorylation status of ERα on Ser167 and Akt on Thr308 by similar mechanisms reported previously; however, we could not find any changes in MAP-kinase factors. Comprehensive phosphoproteomic analysis also indicated the possible contribution of the Akt pathway to the phosphorylation of ERα.

On the other hand, constitutive activation of c-Jun N-terminal kinase (JNK) was observed in ERE-GFP-negative EDR cells, and the growth of these cells was inhibited by a JNK inhibitor. An IGF1R-specific inhibitor diminished the phosphorylation of JNK, which suggested that a novel signaling pathway, IGF1R-JNK, may be important for the proliferation of ER-independent MCF-7 cells. These results indicate that ER-positive breast cancer cells can acquire resistance by more than two mechanisms at a time, which suggests that multiple mechanisms may occur simultaneously. This finding also implies that breast cancers with different resistance mechanisms can concomitantly occur and mingle in an individual patient, and may be a cause of the recurrence of cancer.

1. Introduction

Estrogen plays a pivotal role in the development and progression of breast cancers. It exerts its effects by binding to estrogen receptor α (ERα). This complex then interacts with estrogen response element (ERE) and regulates the transcription of target genes controlling proliferation and cell survival. Therefore, blockade of the estrogen signal is an important strategy for ERα-positive breast cancers. Aromatase inhibitors (AI) that inhibit the biosynthesis of estrogen and antiestrogens that compete for binding to ER have improved the prognosis of patients. Approximately 70% of breast cancer cases have ERα-expressing tumors; therefore, they can be candidates for hormonal therapy targeting ERα. Since hormonal therapy is very effective for ER-positive breast cancer patients without severe adverse events, it is widely used not only in advanced cancer, but also in an adjuvant setting [1]. However, more than a few patients relapse. Therefore, numerous studies on hormonal therapy resistance have been undertaken, especially on tamoxifen

Abbreviations: EDR, estrogen-deprivation-resistant; LTED, long-term estrogen-depleted.

* Corresponding author at: Department of Molecular and Functional Dynamics, Tohoku University Graduate School of Medicine, Aoba-ku, Sendai 980-8575, Japan.
E-mail address: shin@med.tohoku.ac.jp (S.-i. Hayashi).

[1] These authors contributed equally to this work.

0960-0760/$ – see front matter © 2013 Elsevier Ltd. All rights reserved.
http://dx.doi.org/10.1016/j.jsbmb.2013.08.012

resistance [2]. Aromatase inhibitors have recently replaced antiestrogens as a more appropriate hormonal therapy for advanced breast cancer and also in an adjuvant setting [3]. Although estrogen ablation is another effective strategy for ER-positive breast cancer, the acquisition of estrogen-deprivation resistance is one of the crucial steps in the progression to hormonal therapy resistance and more aggressive tumors in ERα-expressing breast cancer. The mechanisms for the estrogen-deprivation resistance of ERα-expressing breast cancer cells have also been explored by several laboratories [4–6] using whole cells cultured for a long-term period in estrogen-deprivation medium. These reports suggested that resistant cells acquired estrogen hypersensitivity by crosstalk with the MAP-kinase or PI3K-Akt pathway and the involvement of membrane-associated ER [7]. However, the precise mechanisms are not fully understood, and several questions remain unanswered in terms of whether any other mechanisms are associated with this resistance. To address these issues, we here established several MCF-7 cell sub-lines by isolating single colonies under long-term estrogen-deprivation conditions. MCF-7 cells stably transfected with the ERE-GFP reporter gene were used as parental cells for this cell cloning. These cells expressed GFP on ER activation, and ER activity was assessed in living cells by fluorescence [8,9]. Using this system, we eventually established the two types of clones as long-term estrogen depletion resistant (EDR) cell lines and characterized them. Our study indicated that more than two clearly distinct mechanisms exist in estrogen-deprivation resistance.

2. Materials and methods

2.1. Reagents

Estradiol (E2) and 4-hydroxytamoxifen were purchased from Sigma–Aldrich (St. Louis, MO, USA). Fulvestrant (Ful) and toremifene (TOR) were kindly provided by AstraZeneca Pharmaceuticals (London, UK) and Nippon Kayaku Co. Ltd. (Tokyo, Japan), respectively. The sources of antibodies for Western blotting were as follows: total ERα (H-184) from Santa Cruz Biotechnology Inc. (Santa Cruz, CA, USA), HER2 from DakoCytomation (Glostrup, Denmark), EGFR, phospho-ERα (Ser167), phospho-ERα (Ser118), total and phospho-p44/42 MAPK (Erk1/2), total and phospho-Akt (Thr308), total and phospho-JNK, β-tubulin, and the PI3K inhibitor, LY294002 from Cell Signaling Technology Inc. (Danvers, MA, USA). Secondary antibodies conjugated with alkaline phosphatase were purchased from Bio-Rad Laboratories Inc. (Hercules, CA, USA). The JNK inhibitor, SP600125, IGF-1R inhibitor, AG1024, and EGFR inhibitor, AG1478, were purchased from Cayman Chemical Company (Ann Arbor, MI, USA) or EMD Biosciences, Inc. (La Jolla, CA, USA).

2.2. Cells and cell culture

MCF-7-E10 cells were established from human breast cancer MCF-7 cells, into which the ERE-GFP reporter gene had been stably introduced. These cells expressed GFP in the presence of estrogen under fluorescence. MCF-7-E10 cells were routinely cultured in RPMI1640 medium (Sigma–Aldrich) containing 10% fetal calf serum (FCS; Tissue Culture Biologicals, Turale, CA, USA) and 1% penicillin/streptomycin (Sigma–Aldrich).

MCF-7-E10 cells were cultured in estrogen-deprived medium for 3 months. Among the surviving cells, ERE-GFP-expressing colonies and ERE-GFP-negative colonies were picked up separately and established as long-term estrogen-deprivation-resistant (EDR) cell lines. EDR cells were maintained in phenol red-free RPMI1640 medium (GIBCO BRL, Grand Island, NY, USA) supplemented with 10% dextran-coated charcoal-treated FCS (DCC-FCS) and 1% penicillin/streptomycin. All cells were incubated at 37 °C in a humidified atmosphere of 5% CO_2 in air. The characteristics of these cells did not change with the number of passages and cells that had gone through as low a number of passages as possible were used in the experiments of this study.

2.3. ERE-GFP assay

We assessed ERE activation by estimating GFP expression levels as reported previously [8–10]. Briefly, the number of cells expressing GFP was counted under fluorescence microscopy after the cells had been harvested by treatment with trypsin. Cells expressing strong levels of GFP were counted. ERE activity were expressed as the percentage of cells expressing GFP.

2.4. Cell growth assay

MCF-7-E10 cells (which had previously been stripped of steroids for 3 days by DCC-FCS-containing medium) and EDR cells were seeded at a density of 5×10^3 cells per well in a 24-well culture plate treated with the indicated concentrations of E2 for 4 days. Cells were counted using a CDA-500 Sysmex automated cell counter (Sysmex Corp., Kobe, Japan). Data are indicated as values relative to the cell numbers of the vehicle-treated control.

2.5. Real-time PCR

Total RNA was extracted from whole cells using Isogen (Nippon Gene Co., Ltd., Toyama, Japan) according to the manufacturer's instructions. Extracted RNA (1 μg) was converted to first-strand cDNA primed with a random hexamer in a 10 μl reaction volume using an RNA PCR kit (Takara Bio Inc., Otsu, Japan) and a 2 μl aliquot was used as a template for real-time PCR. All RNA quantification was carried out according to the standard protocol on an Applied Biosystems Step One real-time PCR system (Applied Biosystems Inc., Foster City, CA, USA). Target gene expression was normalized to *glyceraldehyde-3-phosphate dehydrogenase (GAPDH)*. All PCRs were performed at least twice and the results shown were from samples analyzed in triplicate in one experiment. These results confirmed the reproducibility of the data obtained. The sequences of the primer sets were as follows: *EGR3*-forward, 5′-GAG CAG TTT GCT AAA CCA AC-3′; reverse, 5′-AGA CCG ATG TCC ATT ACA TT-3′; *pS2*-forward, 5′-TCC CCT GGT GCT TCT ATC CTA A-3′; reverse, 5′-ACT AAT CAC CGT GCT GGG GA-3′; *PgR*-forward, 5′-AGC TCA CAG CGT TTC TAT CA-3′; reverse, 5′-CGG GAC TGG ATA AAT GTA TTC-3′; *Bcl-2*-forward, 5′-GTG GAT GAC TGA GTA CCT GAA C-3′; reverse, 5′-GCC AGG AGA AAT CAA ACA-3′; *CyclinD1*-forward, 5′-GGA GCC CGT GAA AAA GAG-3′; reverse, 5′-CAG GTT CCA CTT GAG CTT GT-3′; *GAPDH*-forward, 5′–ACA TCG CTC AGA CAC CAT GG-3′; reverse, 5′–GTA GTT GAG GTC AAT GAA GGG-3′.

2.6. Western blot analysis

Cell lysates were prepared using Lysis-M Reagent (Roche Diagnostics GmbH, Mannheim, Germany) supplemented with phosphatase inhibitor cocktails, Phos STOP (Roche Diagnostics), according to the manufacturer's instructions. Total proteins were run on SDS-PAGE using 10% acrylamide gels (SuperSep™ ace; Wako Pure Chemical Industries, Ltd., Osaka, Japan) and proteins were transferred to PVDF, Amersham Hybond™-P (GE Healthcare UK, Ltd., UK). The expression of proteins was determined by Western blotting with specific antibodies listed in *Reagents*, and expression signals using Immun-star AP substrate (Bio-Rad) were obtained by enhanced chemiluminescence. Densitometry was performed on three blots (two blots only in Fig. 4A) and these results

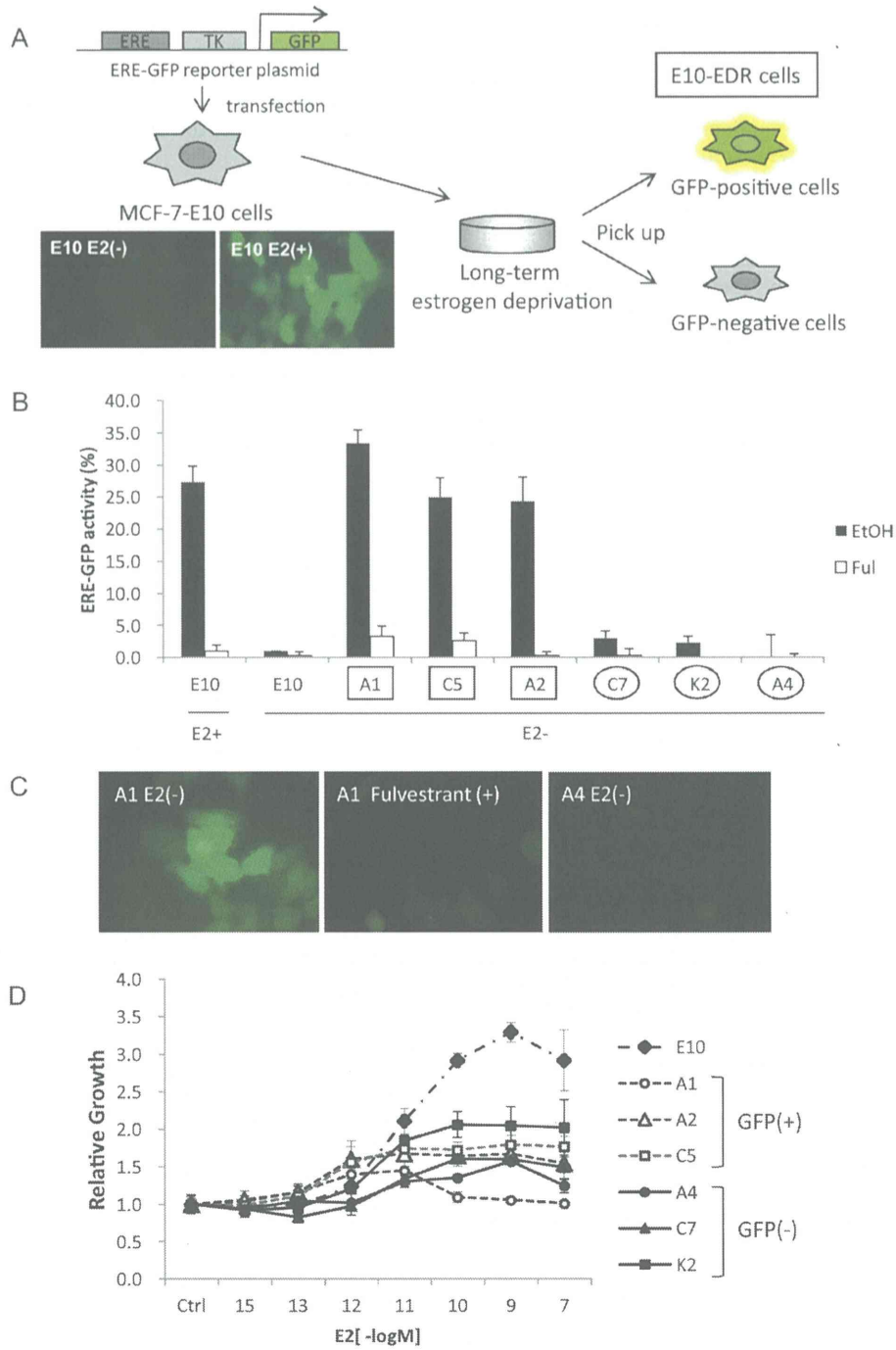

Fig. 1. Establishment of E10-EDR (estrogen-deprivation-resistant) cells. (A) MCF-7-E10 cells were cultured in RPMI1640 with 10% DCC-FCS for at least 3 months. Among the surviving cells, GFP-positive and GFP-negative colonies were isolated and established as long-term estrogen-deprivation-resistant (EDR) cell lines. (B) E10 and the isolated clones were treated with or without a pure antiestrogen (1 μM fulvestrant) in estrogen-deprived medium (E2−) and screened by counting the number of GFP-expressing cells. For comparison, E10 was performed with the same treatment in estrogen condition medium (E2+). As representative clones, three clones (A1, A2, C5) with high GFP expression and another three clones (A4, C7, K2) that did not show GFP expression were used for the following experiments. All data shown are means ± SD of these independent experiments. (C) Pictures of EDR cells under fluorescence microscopy. Examples of GFP-positive cells, A1 and treated with fulvestrant (1 μM) and GFP-negative cells A4 in the absence of estrogen. (D) EDR cells exhibited estrogen-independent growth. After 3 days of culture in RPMI1640 with 10% DCC-FCS, MCF-E10 and EDR cells were plated at 5×10^3 cells/well into 24-well plates and cultured in estrogen-deprived medium including a series of estrogen concentrations for 4 days. The number of cells was counted using a Coulter Counter. Data are indicated as values relative to the cell numbers with vehicle because the condition in which each cell can exhibit stationary proliferation is better as the control. All data are shown as means ± SD of three independent experiments.

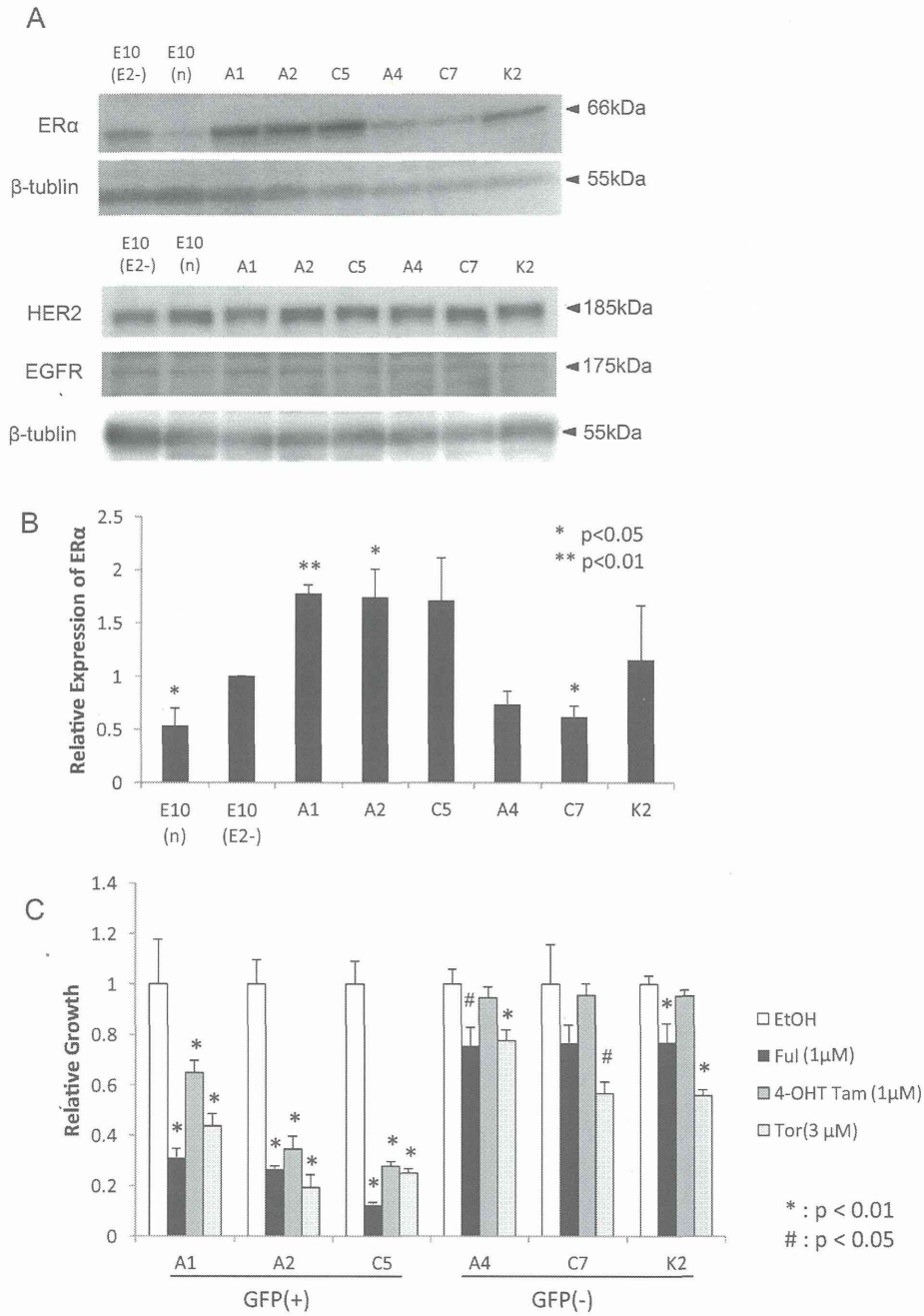

Fig. 2. Characterization of EDR cells. (A) Western blot analysis using whole-cell lysates from MCF-7-E10 and EDR cells was performed using antibodies against ERα, HER2, EGFR, and β-tubulin as described in Section 2. (B) Densitometry results on ERα blots. Densitometry was performed on three blots and the results were indicated as values relative to the intensity with E10 (E2−). Statistical analysis of the indicated averages was performed using the Student's *t*-test, $p < 0.01$ and $p < 0.05$. (C) Effect of antiestrogens on EDR cells. EDR cells (plated 1×10^4 cells/well into 24-well plate) were cultured in RPMI1640 with 10% DCC-FCS. The cells were incubated with the antiestrogen drugs, 1 μM fulvestrant (Ful), 1 μM 4-hydroxytamoxifen (4-OHT), and 3 μM toremifene (Tor) with ethanol (EtOH) as a control. The concentrations of antiestrogens were based on the concentration in the blood or tissue using a clinical dose. The number of cells was estimated after 4 days as described in Section 2. Data are indicated as values relative to the cell numbers with vehicle. All data are shown as means ± SD of three independent experiments.

are shown in figures, which indicated values as relative to the intensity obtained with E10 (E2−) or the controls as one.

2.7. AP-1 luciferase assay

AP-1 activity in MCF-7-E10 cells and EDR-E10 cells was measured using plasmids containing the AP-1 responsive element (TAAAAAAGCATGAGTCAGACACCTGAGCT) upstream of the collagenase gene in the pGL-2-promoter vector (Promega, Madison, WI, USA) and Dual-Luciferase Reporter System (Promega, Madison, WI, USA). MCF-7-E10 cells and EDR cells were seeded at a density of 5×10^4 cells per 6-cm dish in estrogen-deprived medium and cultured for 24 h. The AP-1-Luci plasmid (0.5 μg) and pRL-Luci plasmid (0.05 μg) were mixed with 5 μl of TransIT LT-1 reagent (Takara Bio

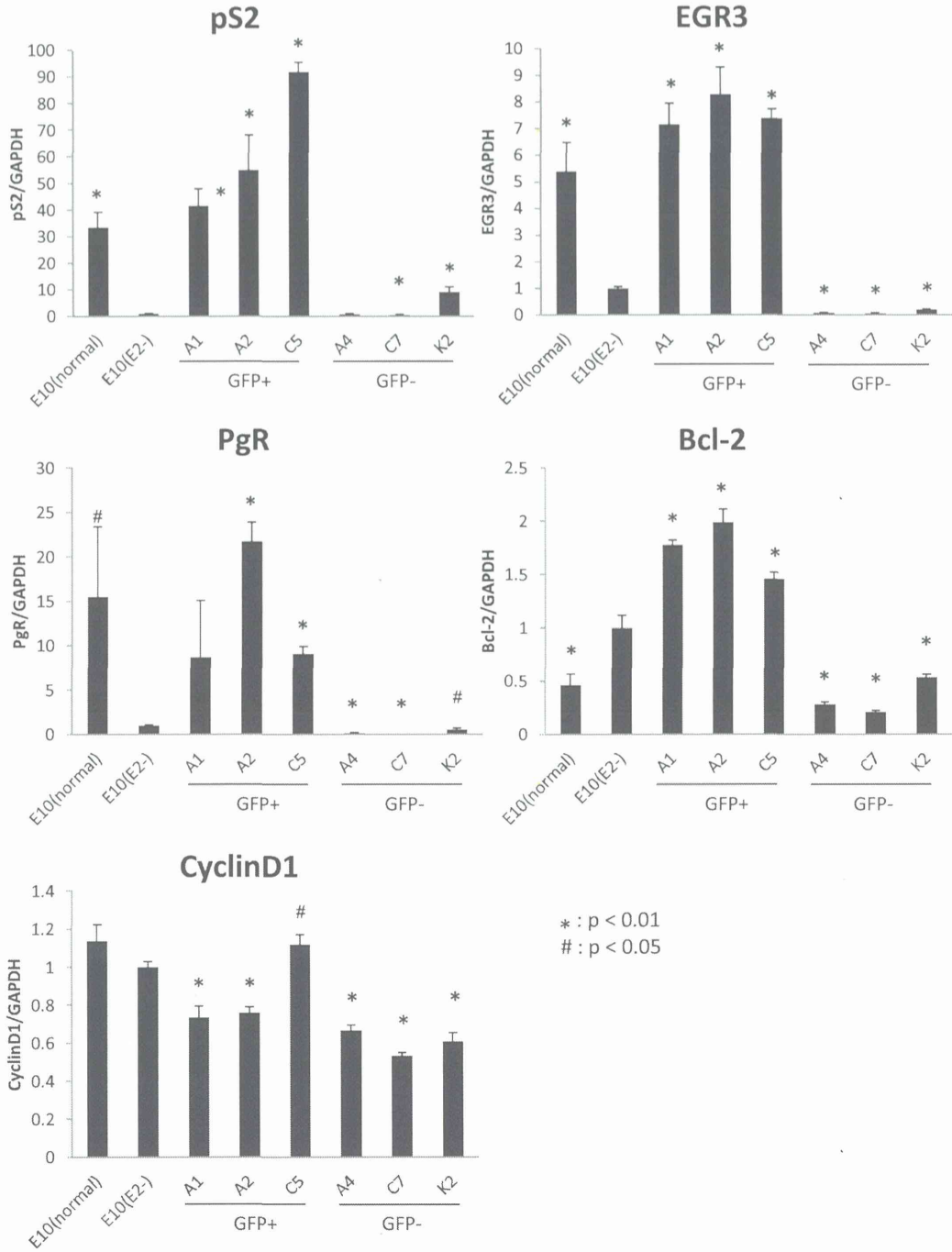

Fig. 3. The expression of ER-target genes. *pS2*, *EGR3*, *cyclinD1*, *progesterone receptor (PgR)*, and *Bcl-2* were measured by real-time PCR normalized to glyceraldehyde-3-phosphate dehydrogenase (GAPDH) in MCF-7-E10 and EDR cells. Total RNA extracted from MCF-7-E10 was cultured in normal RPMI1640 with 10% FCS (normal) or RPMI1640 with 10% DCC-FCS (E2−), and EDR cells was cultured in RPMI1640 with 10% DCC-FCS (E2−). Statistical analysis of the indicated averages was performed using the Student's *t*-test where $p < 0.05$ (#) or $p < 0.01$ (*) indicated a significant difference from E10 (E2−).

Inc.) in 300 μl of serum-free medium and subjected to transfection for 24 h. Luciferase activity was measured according to the manufacturer's instructions using the Dual-Luciferase Reporter Assay System (Promega).

2.8. GAL-4 reporter assay

The transcriptional activity of the A/B and E domains in ER was analyzed by luciferase assays using pCMX-GAL4-N-ER.A/B and pCMX-GAL4-N-ER.E expression plasmids, which contained a sequence encoding either the ER.A/B or ER.E region of ERα fused to the GAL4 DNA binding domain [11]. MCF-7-E10 cells and EDR cells were seeded at a density of 5×10^4 cells per 6-cm dish in estrogen-deprived medium and cultured for 24 h. After co-transfection with 0.05 μg of pCMX-GAL4-N-ER.A/B, 0.5 μg of tk-GALpx3-Luc, or 0.05 μg of the pRL-TK-Luc control plasmid with 5 μl of TransIT LT-1 reagent in DCC-FCS medium for 1 h, cells were treated with LY294002 (5 μM) and cultured for 24 h. Luciferase

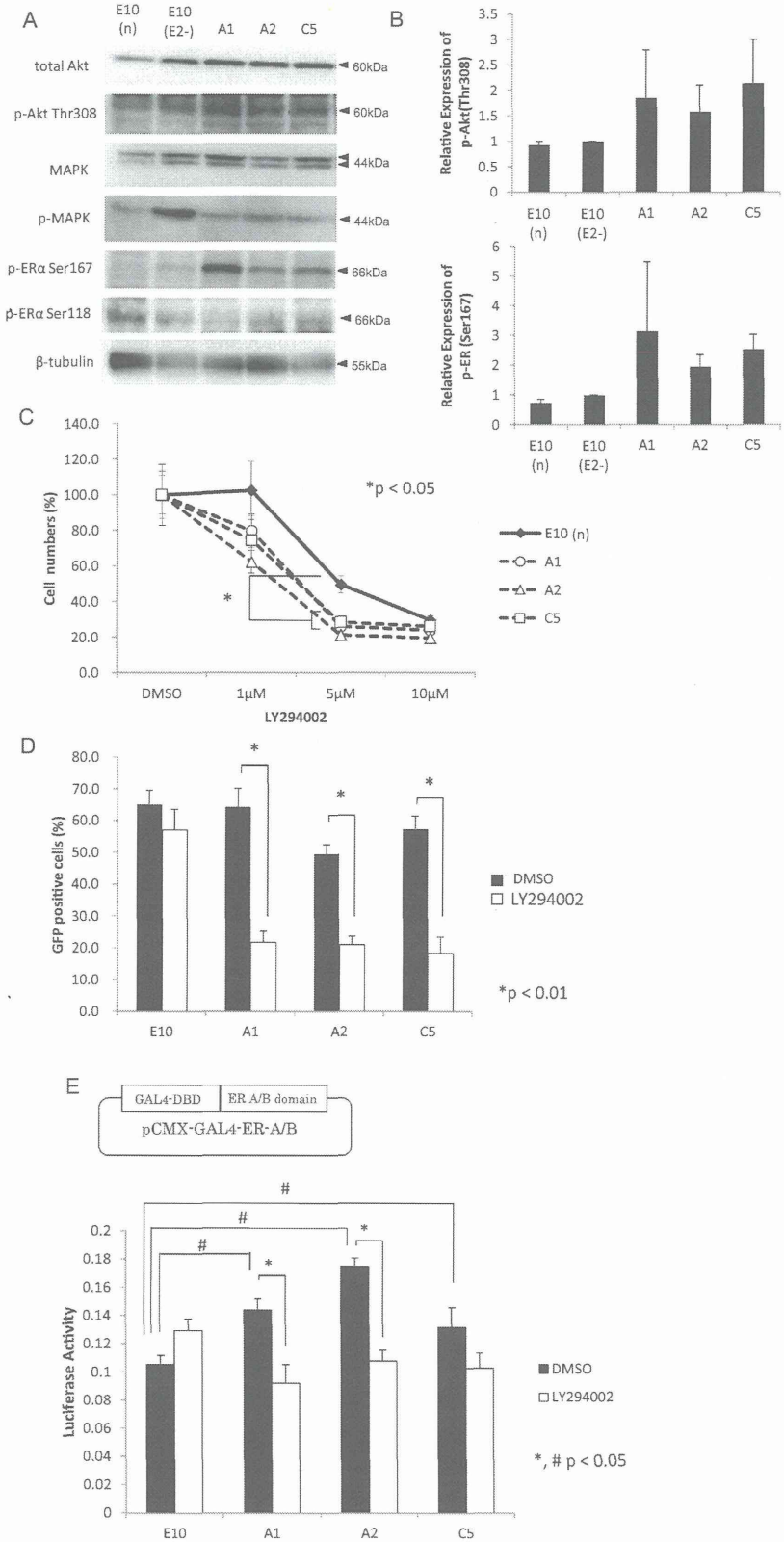

Fig. 4. The mechanisms of constitutive ER activation in GFP-positive EDR cells. (A) Western blot analysis using whole-cell lysates from MCF-7-E10 cells, which were cultured with RPMI1640 with 10% FCS (normal; *n*) or RPMI1640 with 10% DCC-FCS (E2−), as well as EDR cells, was performed using antibodies against total Erk1/2, p-Erk1/2, total Akt, p-Akt (Thr308), p-ERα (Ser167), p-ERα (Ser118), and β-tubulin as described in Section 2. (B) Densitometry results on p-Akt (Thr308) and p-ERα (Ser167) blots. Densitometry was performed on blots and the results were indicated as average values relative to the intensity with E10 (E2−). (C) The growth of GFP-positive cells was inhibited by the PI3K inhibitor. MCF-7-E10 cells were plated at 1.0×10^4 cells/well into a 24-well plate and were cultured in RPMI1640 with 10% FCS (normal). EDR cells (A1, A2, C5) were also plated at 1.0×10^4 cells/well into a 24-well plate and were cultured in RPMI1640 with 10% DCC-FCS. We set each medium so that E10 and EDR cells could proliferate

activity was measured twice and normalized with pRL-TK-Luc activity.

2.9. Mass spectrometry-based phosphoproteome analysis and KeyMolnet analysis

MCF-7-E10 cells and EDR cells (A1) were cultured in RPMI1640 with 10% FCS or phenol red-free RPMI1640 with 10% DCC-FCS, respectively, and cell lysates were harvested. Sample preparation for mass spectrometric analyses (i.e., cell lysate, protein extraction, protein digestion, phosphopeptide enrichment) was performed as described elsewhere [12]. Purified samples were then analyzed using an LTQ-Orbitrap mass spectrometer (Thermo Fisher Scientific, Waltham, MA, USA) [13]. Peptides and proteins were identified by means of an automated database search using Mascot version 2.2 (Matrix Science, London, UK) against UniProt/SwissProt release 56.0 with a precursor mass tolerance of 3 ppm, fragment ion mass tolerance of 0.8 Da, and strict trypsin specificity allowing for up to two missed cleavages. Cysteine carbamidomethylation was set as a fixed modification, and methionine oxidation and the phosphorylation of serine, threonine, and tyrosine were allowed as variable modifications. Peptides were considered to be identical if the Mascot score was over the 95% confidence limit based on the "identity" score of each peptide, and at least three successive y or b ions with two and more y, b, and/or precursor origin neutral loss ions were observed. Phosphorylated sites were unambiguously determined when y or b ions, between which the phosphorylated residue was located, were observed in the peak lists of the fragment ions. Phosphorylated peptides were measured and identified by LC–MS/MS. We extracted phosphorylated peptides that exceeded 10,000 in the peak area value of A1 (ERE-GFP-positive cell) and picked up those that were 5-fold over the A1/MCF-7-E10 cell value (Supplemental Table 1). Phosphoproteomic data were analyzed by KeyMolnet software, which is a new approach to mechanistic analysis and was developed by the Institute of Medicinal Molecular Design, Inc. (IMMD) [14]. Known molecular data and our phosphoproteomic data were combined with this software and shown as a molecular network. We performed a "start point to end point search" by selecting phosphorylated peptides identified by proteomics as starting points and estrogen receptor alpha as an end point.

Supplementary material related to this article can be found, in the online version, at http://dx.doi.org/10.1016/j.jsbmb.2013.08.012.

2.10. Statistical analyses

The Student's *t*-test was used to assess the significance of differences between two groups performed in triplicate. Data were expressed as means ± SD. $p < 0.05$ was considered significant.

3. Results

3.1. Establishment of estrogen-deprivation-resistant ERE-GFP-positive and negative MCF-7 cell lines

MCF7-E10 cells that had been stably transfected with the ERE-GFP reporter plasmid [8] were used as the parental cells to isolate estrogen-deprivation-resistant MCF-7 cells. They were cultured in DCC-treated FCS medium for at least 3 months. Among the surviving cells, ERE-GFP-expressing colonies and ERE-GFP-non-expressing colonies in the estrogen-deprivation (ED) medium were separately picked up (37 colonies) under a fluorescent microscope (Fig. 1A), and several cell lines (10 clones) were established by subsequent culture and passage in ED medium. The ERE-GFP activities of these established cell lines were analyzed according to the previously described method [8–10]. Fig. 1B shows representative examples of the activity of each of these EDR ERE-GFP-positive and ERE-GFP-negative MCF7-E10 cells. Three clones (A1, A2, C5) that had higher activity than the others and another three clones (A4, C7, K2) that showed almost no ERE-GFP activity were selected and used for the following experiments. ERE-GFP activity was strongly inhibited by the addition of the pure antiestrogen fulvestrant, which indicated the involvement of ERα in the activity of these ERE-GFP-expressing cells (Fig. 1B and C). In addition, the conventional ERE-luciferase assay of these EDR-MCF-7 cells also showed high ER activity in GFP-positive cells, but low activity in GFP-negative cells (Supplemental Data 1). The estrogen dependence of cell growth in these EDR-MCF7-E10 cells was then analyzed. Both ERE-GFP-positive and -negative EDR cells showed much lower sensitivity to estrogen than parental cells (Fig. 1D).

Supplementary material related to this article can be found, in the online version, at http://dx.doi.org/10.1016/j.jsbmb.2013.08.012.

3.2. Overexpression of ERα in GFP-positive EDR-MCF7-E10 cells

ERα protein expression in these cell lines revealed the significant induction of ERα expression in all three ERE-GFP-positive cell lines (Fig. 2A and B). Previous reports showed the induction of human epidermal growth factor receptor type 2 (Her2) and epidermal growth factor receptor (EGFR) expression in estrogen-deprivation-resistant cells [15,16]. However, none of our EDR-MCF-7-E10 cell lines showed the significant up-regulation of Her2 or EGFR expression (Fig. 2A).

3.3. Effect of antiestrogens on EDR cells

The effect of antiestrogens on the cell growth of these EDR cells was evaluated as shown in Fig. 2C. The growth of A1, A2, and C5 was inhibited by all antiestrogens, while that of A4, C7 and K2 was not inhibited by 4-OHT. A4 and K2 cell growth was inhibited by fulvestrant, which suggested that it had a stronger effect on the proliferation of these cells than that of tamoxifen. Interestingly, the growth of all ERE-GFP negative cells was significantly diminished by toremifene. These results indicate that ERE-GFP-positive EDR cells were responsive to antiestrogens for hormonal therapy. In contrast, the effect of these drugs was weaker in ERE-GFP-negative ones than in ERE-GFP-positive EDR cells.

3.4. Expression of endogenous ER-target genes in EDR cells

The expression of the endogenous ERα target genes, *pS2*, *PgR*, *EGR3* [17], *Bcl-2* and *CyclinD1* was analyzed by real-time RT-PCR in these cell lines. As shown in Fig. 3, ERE-GFP-positive cells

regularly because E10 was difficult to grow in estrogen-deprived medium. Cells were treated with the PI3K inhibitor, LY294002 (DMSO, 1 μM, 5 μM, 10 μM), for 4 days. The number of cells was counted using a Coulter Counter. All data shown as a percentage of the control are means ± SD of triplicate determinations of three independent experiments. (D) The ER activity of GFP-positive cells was inhibited by the PI3K inhibitor. Cells were cultured as mentioned above for (C), and treated with LY294002 (5 μM) for 4 days. The number of cells expressing GFP was counted under fluorescence microscopy. Data are shown as a percentage of GFP-positive cells among 100 counted cells. (E) ER.A/B-dependent transcriptional activities treated with LY294002 in MCF-7-E10 cells and GFP-positive EDR cells. MCF-7-E10 cells and EDR cells were seeded at a density of 5×10^4 cells per 6-cm dish in estrogen-deprived medium and cultured for 24 h. After the co-transfection of the pCMX-GAL4-N-ER.A/B, tk-GALpx3-Luc, or pRL-TK-Luc control plasmid in DCC-FCS medium for 1 h, cells were treated with LY294002 (5 μM) and cultured for 24 h. Cell lysates were assayed for luciferase activity. Statistical analysis of the indicated averages was performed using the Student's *t*-test where $p < 0.05$ (B and D), $p < 0.01$ (C).